***Submitted: 08.05.2023.***

***Accepted for publication: 15.05.2023.***

# The influence of printing orientation on the flexural strength of PA 12 specimens produced by SLS

**Ivana Jevtić[1,*], Goran Mladenović[2], Aleksa Milovanović[1], Isaak Trajković[1], Marija Đurković[3], Nenad Korolija[4], Miloš Milošević[1]**

[1]Innovation Center of the Faculty of Mechanical Engineering, Kraljice Marije 16,11120, Belgrade, Serbia.
[2]University of Belgrade, Faculty of Mechanical Engineering, Kraljice Marije 16,11120, Belgrade, Serbia
[3]University of Belgrade - Faculty of Forestry, Kneza Viseslava 1, 11030, Belgrade, Serbia
[4]University of Belgrade - School of Electrical Engineering, The Department of Computer Science and Information Technology,11000 Belgrade, Serbia

*Ivana Jevtic, ijevtic@mas.bg.ac.rs

https://doi.org/10.2298/SOS230508031J

***Abstract:***

*This article aims to investigate the mechanical characteristics of specimens fabricated using Selective Laser Sintering technology. The research covers flexural specimens, produced by PA12 materials. CAD model dimensions were selected according to the ISO 178 standard, and the chosen specimen geometry is 96 x 8 x 4 [mm] in bulk. All specimens were produced using a specialized machine Fuse 1 (FormLabs, Summerville, MA). Four specimen batches were produced, each with a different printing orientation (i.e. vertical and horizontal) and location on the printing plate (i.e. in the middle and on the edge of the powder bed). The specimens are tested using a Shimadzu universal machine for testing the mechanical characteristics of materials, AGS-X 100 kN, with a unique additional tool for testing 3-point bending specimens.*

***Keywords:*** *Selective Laser Sintering; Polyamide 12; 3-point bending; Printing orientation, Flexural strength.*

## 1. Introduction

Additive manufacturing (AM), which used to be called rapid prototyping, nowadays also known as 3D printing, began to be applied in the 80s of the 20th century [1-3]. In the past period, the development of the 3D printing technology has progressed a lot. 3D technologies are commercially available and offer a wide range of possibilities in all areas. Compared to conventional technologies, 3D printing offers advantages in the engineering process. In contrast to conventional methods, which create the final product by removing material, additive manufacturing creates the product by layering the material. [2, 4-7].

The use of 3D printing in production has made it possible to create complex shapes that are very difficult to obtain with conventional production processes. It also has the potential for a faster production time, lower costs and higher efficiency. In addition, 3D printing can be used to reduce

waste, as the process requires only the necessary material to produce the desired product. The 3D printing technology has revolutionized many industries and expanded the possibilities of what can be achieved. 3D printing is continuing to be explored and utilized in various fields, from healthcare to aerospace, and its potentials are still being discovered [7-9].

A wide range of AM processes may be classified according to several parameters, ranging from application to the initial condition of the treated materials or the physical principle underlying the layered solidification process [10, 11]. There are seven types of AM, i.e., 3D printing technologies that use materials with different combinations of the properties of conventional materials [5, 12, 13]. These include: (1) Fused Deposition Modeling (FDM): Which uses thermoplastic polymers as the material and a heated nozzle to extrude a filament onto a build platform; (2) Stereolithography (SLA): Which utilizes a liquid photopolymer that is selectively cured by a UV laser or other light source; (3) Selective Laser Sintering (SLS): Employs a laser to selectively fuse small thermoplastic or metal powder particles; (4) Direct Metal Laser Sintering (DMLS): Similar to SLS but uses metal powders as the material; (5) Electron Beam Melting (EBM): Uses an electron beam to melt metal powders into a solid structure; (6) Binder Jetting (BJ): A liquid binder fuses small metal, ceramic, or composite powder particles; (7) Laminated Object Manufacturing (LOM): Uses layers of paper, plastic, or metal laminates that are selectively cut and bonded together [5, 14].

Each AM process has unique benefits and applications, making them suitable for a wide range of uses. Examples of AM processes include selective laser sintering, fused deposition modeling, and direct metal laser sintering. These processes involve the use of various materials, such as polymers, ceramics, and metals, which can be heated and solidified in a layer-by-layer fashion to create a finished product [15-17]. Other parameters used to classify AM processes include the type of energy used to heat the material, the layer thickness, the building speed, and the post-processing needed to complete the object [1, 18, 19].

Overall, AM processes are highly customizable and can be tailored to meet a variety of needs. AM processes can create complex parts with high accuracy and repeatability depending on the type of material used and the parameters selected. Additionally, AM processes can be used to produce parts quickly and cost-effectively, making them ideal for prototyping and low-volume production runs.

In this paper, the examination of mechanical characteristics was carried out of a series of 3-point bending performed in four batches of specimens made from polyamide 12 (PA12) material using the Selective Laser Sintering (SLS) technology printing. The specimens were tested for different compression orientations and printing locations in the powder bed. This research aimed to analyze the differences in stress-strain diagrams, flexural strength, and other mechanical properties with horizontal and vertical compression orientations as well as in the powder bed's middle or on-the-edge printing locations. The specimens were tested using a three-point bending machine and the results were analyzed using dedicated software. The results of this study will help to further understand the mechanical properties of materials printed using the SLS technology and how they are affected by different printing orientations and locations in the powder bed.

## 2. Methodology

This chapter is divided into four parts for a better transparency of all segments. In the first part, there was something more to say about the SLS printing technology. This part is followed by sections on the actual preparation of the specimens, as well as on the characteristics of the material used. At the end of the chapter, the testing procedure is described, which includes the machine on which it was tested as well as the characteristics of the machine itself.

### 2.1 SLS technology

SLS is an additive manufacturing technology and a part of the Powder Bed Fusion family which produces 3D objects obtained by joining materials. This material bonding takes place layer by

layer [5,20]. Each of the layers is applied by adding a thin layer of powder, using roller mechanics, over the already bonded part. After that, a laser beam passes over the defined cross-section fusing the selected material into the previous layer [21,22]. As a result, the powder connects horizontally, making a full layer, vertically connecting the preceding layer. Several items of various forms and dimensions can be produced at the same time using the described procedure. The process is followed by post-processing, which entails extracting the model from the unsintered powder solution and sandblasting it. After the post-processing, the real benefit of the SLS technology comes to the fore. Unlike FDM, SLS can 3D print models with complicated geometry without the use of support structures since they are suspended in powder [23].

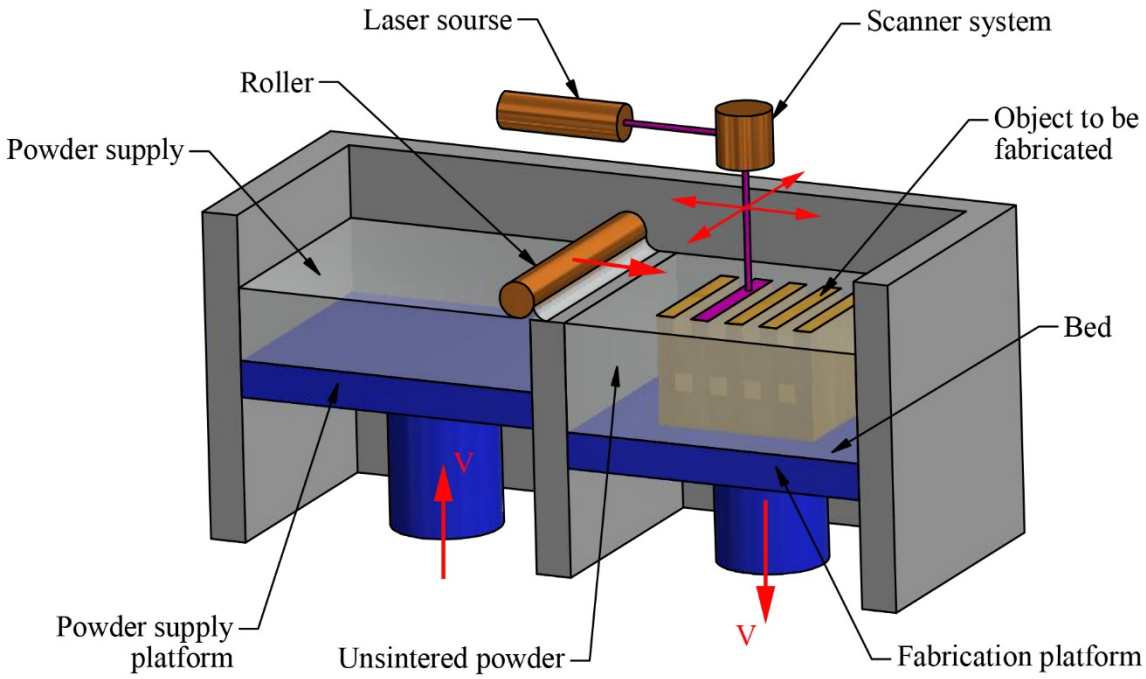


**Fig 1.** Schematic representation of the working principle of the SLS device.

Objects produced with the SLS technology may be made of plastics (mostly polyamide-based), metals (often steel, aluminum, and titanium-based powders), ceramics, and composites [16,17,24,25]. The most commonly commercially available materials used in the SLS technology come in the powder form and include polymers such as polyamides (PA), polystyrenes (PS), thermoplastic elastomers (TPE), and polyaryletherketones (PAEK). Polyamide, in the form of compound PA12, is the most often used material in the SLS technology in commercial systems. This polyamide can be glass-reinforced at times, while compound polyamide PA11 is also utilized.

### 2.2 Specimen preparation – 3D printing

In this research, 3-point bending specimens with the recommended dimensions were created by the ISO 178:2003 standard. Specimen 3D models were created in CAD software (SolidWorks, Dassault Systèmes, Vélizy-Villacoublay, France) saved in the STL format, and then „sliced“ in the PreForm software (Formlabs, Sommerville, MA, USA). The specimen length, height, and thickness are l=96 mm, h=4 mm and b=8 mm, respectively (see Fig 2). According to the standard, the acceptable loading and supporting pin radius for the used specimen size is 5 mm.

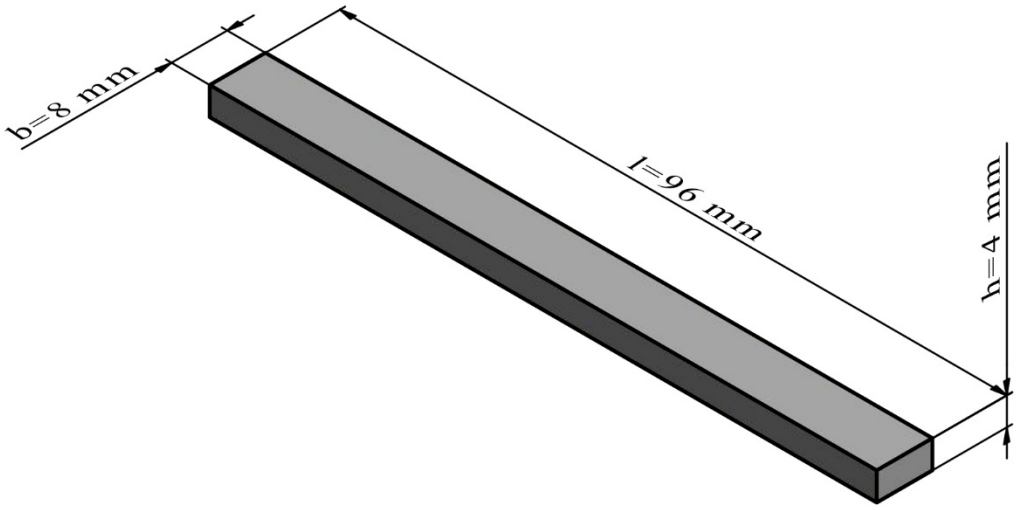


**Fig 2.** 3-point bending specimen dimensions.

Four batches of specimens were printed, with ten specimens in each batch. The batches differed in the printing orientation and printing location. Vertical and horizontal orientations are applied, and each orientation is combined with the printing location, i.e., in the middle and on the edge of the powder bed as shown in Fig 3. Fig 3 shows that HO is horizontally printed specimens on the edge of the powder bed, and HS is horizontally printed specimens in the middle of the powder bed. VO is vertically printed specimens on the edge of the powder bed, while VS is vertically printed specimens in the middle of the powder bed.

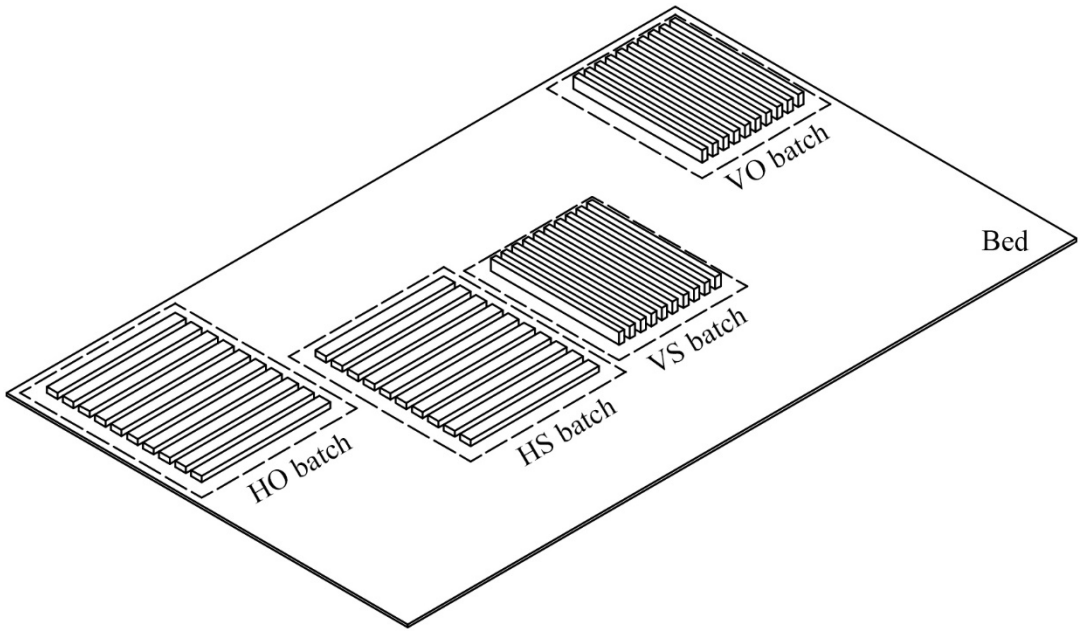


**Fig 3.** Illustration of different specimen orientations and locations on the powder bed.

The specimens were fabricated using selective laser sintering (SLS) technology on the Fuse 1 3D printer (Formlabs, Somerville, Massachusetts). Printing layers are typically 20 to 150 microns thick, while in this research the powder thickness was 110 microns. During printing, all models were at

least 5 mm apart. At a working temperature of 180°C, the laser power of the SLS printer was 63-70 W, while the build volume for this 3D printer is 165x165x300 mm.

During the printing of these specimens, 30% of fresh powder was used, while the rest of the powder was already used during some other printing, i.e. the rest is the so-called sifted powder. Then the powder mixture was poured into a cartridge, which was placed in the machine and mixed for 15 minutes. The old powder was mixed with the new one. After mixing, part of the powder, i.e. 4-5 kg, it was fed into the printer as needed for printing. Then the optical cassette was checked. It contains protection for the camera, as well as protection for the laser itself. After each print, dust remains on the glass protection. If the cassette is not cleaned before use, when the laser is turned on it disperses the remains of that powder, which remains retained on the protective glass. In addition, there is an infrared sensor, which is checked before printing. The parts of that sensor are printed, and sometimes the filters are cleaned before putting them into operation. After printing, when the specimens have cooled, they are cleaned even more thoroughly with a sandblaster. After sandblasting, the specimens were rinsed under a jet of water to remove the powder parts that remained sandblasting. Then the specimens were dried at room temperature and were ready for use.

### 2.3 Materials

The specimens for this research were produced using the PA12 material (Formlabs, Sommerville, MA, USA). One of the materials that are most often used is the one mentioned, both for complex assembly and prototypes. It is a strong, long-lasting material that may be used to make useful parts because of its flexibility, heat resistance, and adequate mechanical qualities [24]. PA12 is commonly used in the automotive, aerospace, and industrial sectors for applications such as gears, bearings, and pump components [25]. The glass transition temperature is around 48.8°C, while the materials' melting point is between 178°C and 180°C, which represents the lowest melting temperature of the material among all polyamides. The properties of PA12 include minimal water absorption, 1.01 $g/cm^3$ density, chemical resistance, and lack of sensitivity to stress cracking [26]. Table 1 shows a review of some of the mechanical properties of PA12.

**Tab. I** Properties of the PA12 material [27].

| **Property** | **Value** |
|---|---|
| Ultimate Tensile Strength | 50 MPa |
| Flexural Strength | 66 MPa |
| Elastic modulus | 1850 MPa |
| Break strain | 11% |

### 2.4 Testing procedure

For this research, a total of forty specimens were printed, divided into four batches of ten specimens each. The batches were distinguished by variations in printing orientation and location. Both vertical and horizontal orientations were utilized, with each orientation paired with a specific printing location - either in the middle or on the edge of the powder bed.

Shimadzu AGS-X universal testing machine (Shimadzu Corp., Kyoto, Japan) was used to perform three-point bending tests. The load cell capacity of this machine is 100kN, with a measurement inconsistency of less than 200 N. The machine may do tensile, compressive, and bending tests depending on the attached adaptors. The specimen was put on two supporting pins spaced apart for three-point bending. In this test, supporting pegs were placed at a predetermined spacing of 70 mm

(Fig. 4). With a precision of ±0.5%, this particular device allows for highly accurate measurements [28]. It is capable of reproducing speeds between 1/1000 mm/min and 800 mm/min with an accuracy of ±0.1%. Given research approach can be extended by using optical systems such as 3D scanners and digital image collection (DIC) techniques. 3D scanners are the most often used for dimensional analysis of polymer and composite materials obtained by additive manufacturing while DIC is used for deformation analysis of simple and complex shapes, due to different types of loading [29-35].

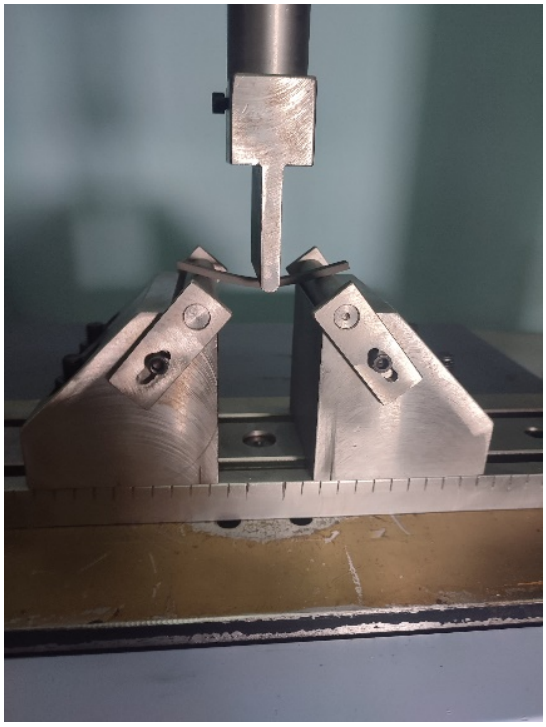

**Fig 4.** Shimadzu AGS-X Universal Testing Machine with a Specimen and 3-Point Bending Test Tool.

In this testing, the sampling rate was set to 100 Hz. Trapezium-X software (Shimadzu Corp., Kyoto, Japan) was used to acquire the results of the 3-point bending tests. Defining the testing method in the aforementioned Trapezium-X software includes defining the strain rate, the dimensions of the specimens and the required output. The 3-point bending test was carried out at a 2 mm/min speed according to the ISO 178:2003 standard. Dimensional discrepancies were within tolerance limits after 3D printing. The thickness and width of the specimens were measured three times and the mean results were utilized for tests.

## 3. Results and discussions

The three-point bending tests were performed according to the ISO178 standard, with ten specimens in each of the four series. In the bending test, the deformation is measured using the formula (1) from the ISO 178 standard:

$$\varepsilon = \left(\frac{6Sh}{L^2}\right) \cdot 100\% \quad (1)$$

where $h$ is the specimen's height, which is approximately 4 mm. $h$ of each specimen was measured before testing until $L$ is the distance between the supporting fixture and which is 70 mm. $S$ is deflection (ISO178:2003,) which is measured as the displacement of the top specimen surface's center point (Fig 5).

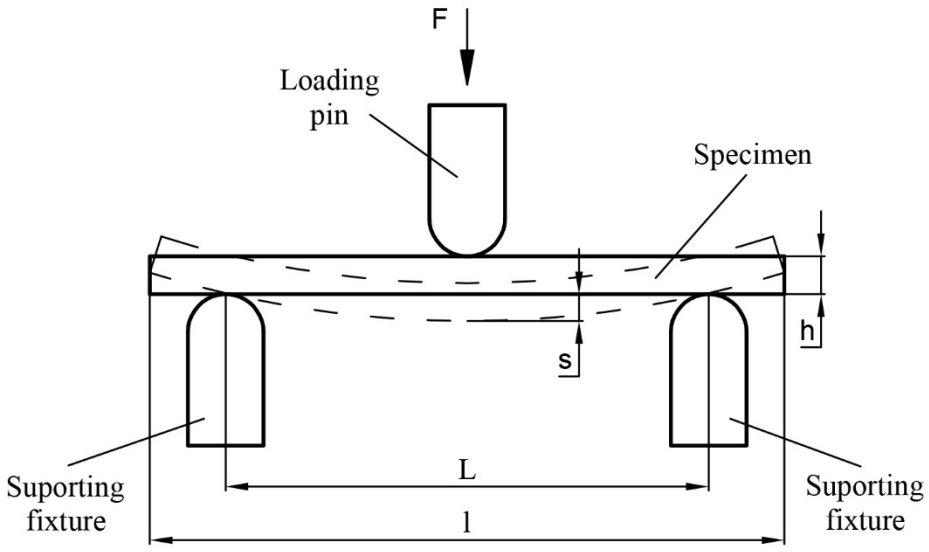


**Fig 5.** Schematic of the three-point bending test.

In three-point bending tests, this point coincides with the loading pin tip. In these tests, the machine controls the position of the loading pin, which represents the measurement of the top surface middle point displacement needed by the formula (1).

Flexural stresses were calculated using the following formula (2):

$$\sigma = \frac{3Fl}{2bh^2} \tag{2}$$

where $b$ is the thickness of the specimens, and its dimension for each specimen was measured after printing and is approximately 8 mm, while $F$ is the measured force value from the universal testing machine's load cell.

The average values of the dimensions of the specimens and the mean value of the force and deflection for each type of the test specimen are given in Table 2.

**Tab. II** Mean values of $h$, $b$, $S$ and $F$ sizes for all types of specimens.

| Specimens | $h$ $[mm]$ | $b$ $[mm]$ | $S$ $[mm]$ | $F$ $[N]$ |
|---|---|---|---|---|
| HO | 3.97 | 7.25 | 13.76 | 82.23 |
| HS | 3.97 | 7.3 | 13.26 | 89.35 |
| VO | 4.05 | 7.45 | 8.29 | 67.29 |
| VS | 4.06 | 7.28 | 8.9 | 74.4 |

Based on the values shown in Table 3 and formulas 1 and 2 obtained from the ISO 178 standard, the values of some mechanical characteristics are obtained. 3-point bending test results (i.e. flexural strength, elongation at flexural strength) for all specimens manufactured specimens are shown in Table 3 and the following diagrams.

**Tab. III** Mechanical properties from the three-point bending test of the tested PA12 material.

| Specimens | Flexural strength [MPa] | Elongation at flexural strength [%] |
|---|---|---|
| HO | 73.93 | 7 |
| HS | 79.9 | 6.65 |
| VO | 55.9 | 4.12 |
| VS | 63.16 | 4.45 |

The results obtained by determining the engineering stress and engineering strain of horizontally and vertically printed specimens on the edge of the powder bed and in the middle of the powder bed are shown below.

Figure 6 shows the result of measurements on specimens of horizontally printed specimens on the edge. The results of the three-point bending test show the highest values for flexural strength and failure stress for specimen HO9, which is 77.21 MPa, while for specimen HO5 that value is 77.09 MPa. The minimum value of engineering stress is about 68 MPa, which is by about 10 MPa lower than the maximum value. The value of engineering strain is in the range from 6.7% to 7.4% for this series of specimens.

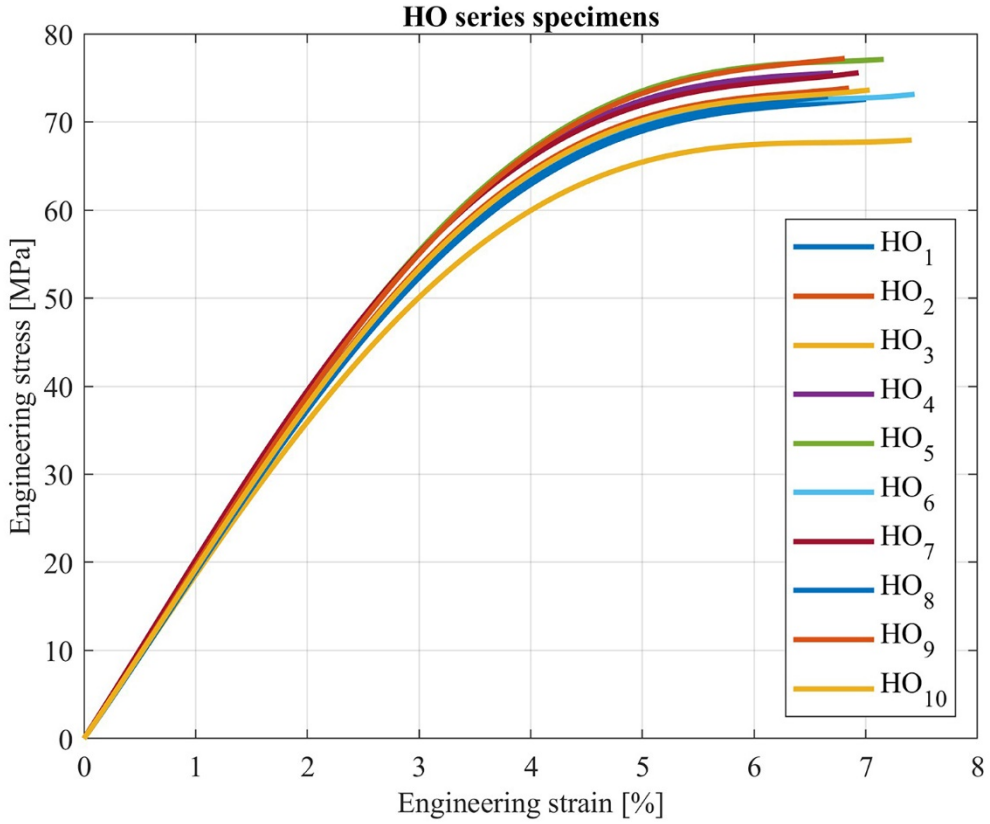


**Fig 6.** Dependence of engineering stress on the engineering strain for HO specimens.

Figure 7 shows that all ten test specimens have approximately the same values of engineering stresses, indicating that the material being tested exhibited consistent behavior under the applied forces. The maximum engineering stress value of 81.5 MPa suggests that the material can withstand a relatively high amount of stress before failure. The engineering strain values, ranging from 6% to 7.3%, indicate that the material underwent moderate amounts of deformation when subjected to the 3-

point bending test. The relationship between stress and strain can provide insights into the material's mechanical behavior, such as its modulus of elasticity or the material's stiffness.

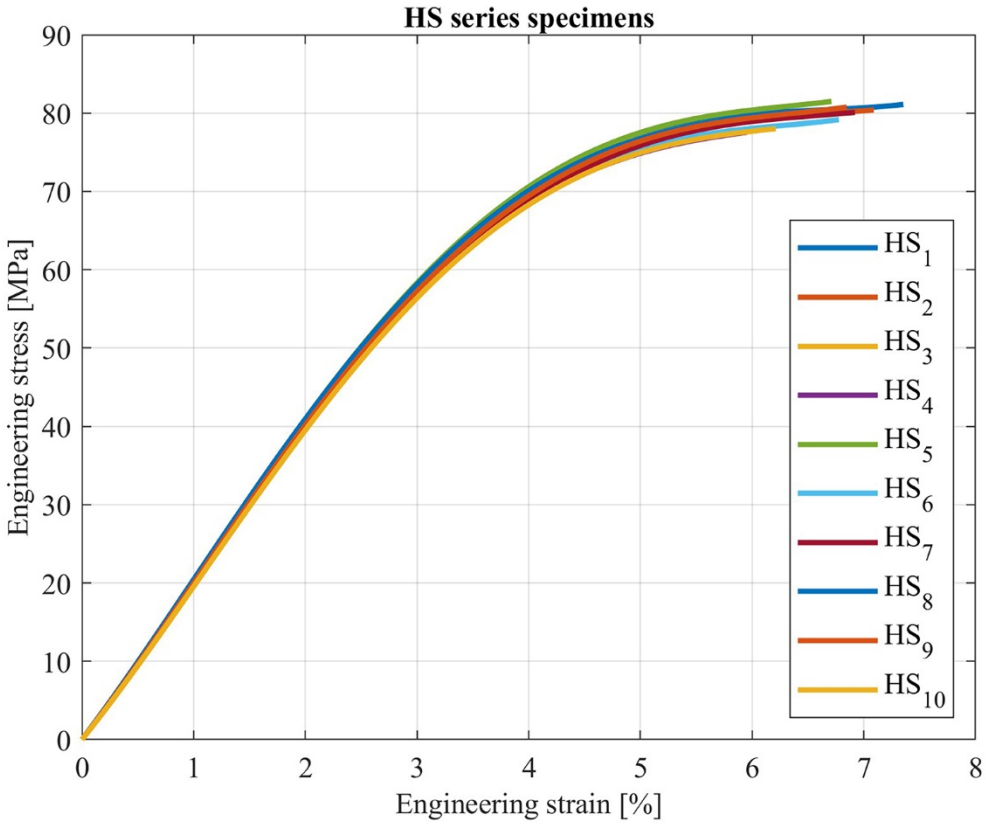


**Fig 7.** Dependence of engineering stress on the engineering strain for HS specimens.

If we compare the diagrams in Figures 6 and 7, it can be concluded that horizontally printed 3-point bending specimens (either on the edge or in the middle of the platform) have similar values of mechanical characteristics. The values of engineering stress and engineering strain are similar. With this type of specimen, there is no significant influence on the place of printing of the specimens.

The characteristics of ten specimens that are printed vertically on the edge of the platforms are shown in Figure 8. The specimens are arranged in three series, with several specimens per series. The arrangement is based on the value of engineering stress and stiffness. The series are differentiated based on the values of engineering stress and stiffness, with each series having different values. The minimum value of engineering stress among the specimens is 50MPa, while the maximum value is 62MPa. The engineering strain values for the specimens range from 3.7% to 4.6%. These values indicate the extent to which the specimens can withstand applied loads and deform under stress.

In addition, it should be pointed out that the arrangement of the series takes into account the stiffness of each specimen as well. Stiffness refers to the ability of a material to resist deformation when subjected to an applied force. The specimens with higher stiffness values will deform less than those with lower stiffness values under the same applied load. Figure 8 presents a graphical illustration of the characteristics of ten specimens, including their engineering stress, stiffness, and engineering strain values, as well as their arrangement into three series based on these values.

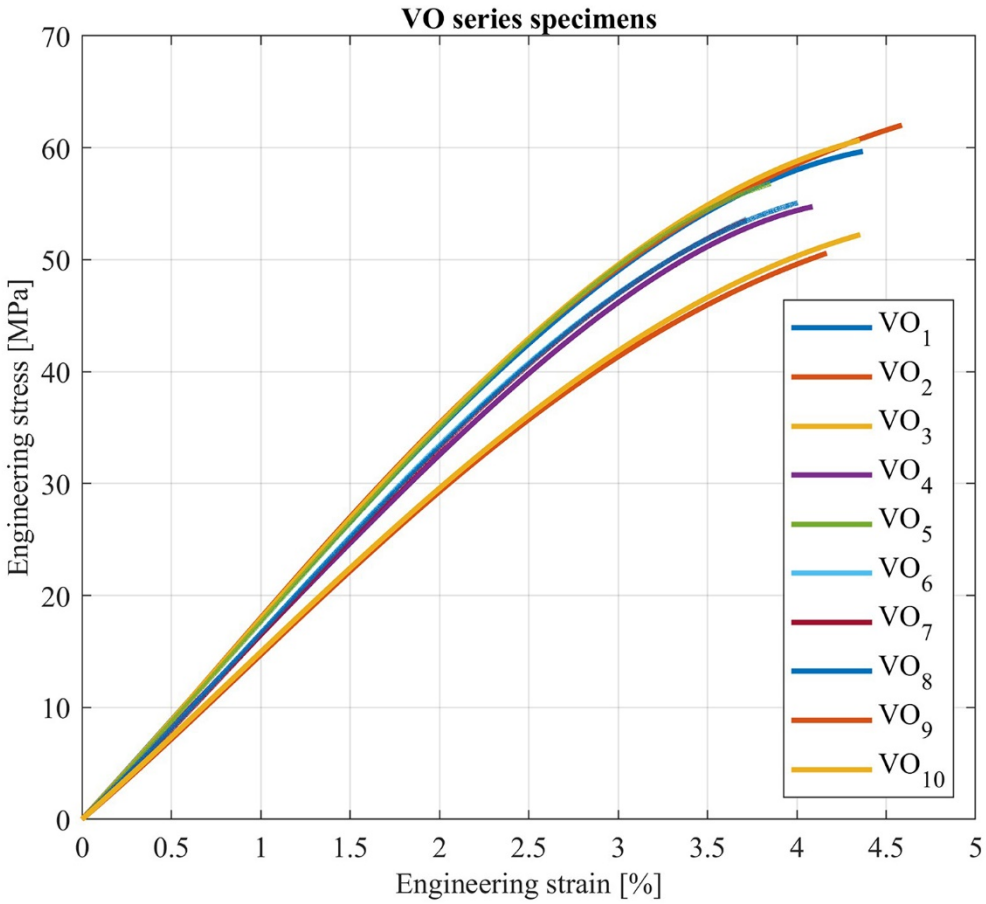


**Fig 8.** Dependence of engineering stress on the engineering strain for VO specimens.

The engineering stress-strain diagram for vertical specimens printed in the middle of the powder bed is depicted in Fig 9. The information provided in Figure 9 suggests that the material being tested had a consistent response to the applied forces, as indicated by the similarity of the engineering stresses observed in all ten test specimens. The maximum engineering stress value of 67 MPa indicates that the material can withstand a relatively high amount of stress before failure, suggesting that it may be suitable for applications where high strength and durability are required.

The engineering strain values observed in the test ranged from 4% to 5%, indicating that the material underwent moderate amounts of deformation when subjected to the 3-point bending test. The relationship between stress and strain can provide valuable insights into the mechanical behavior of a material, including its modulus of elasticity or stiffness. By analyzing this relationship, it may be possible to determine the material's suitability for specific applications or identify potential areas for improvement in its design or manufacture.

Overall, the information provided in Figure 9 suggests that the material being tested exhibited consistent and relatively high levels of strength and durability, with moderate levels of deformation when subjected to external forces. Further analysis of the material's mechanical properties and behavior may provide additional insights into its performance and potential applications.

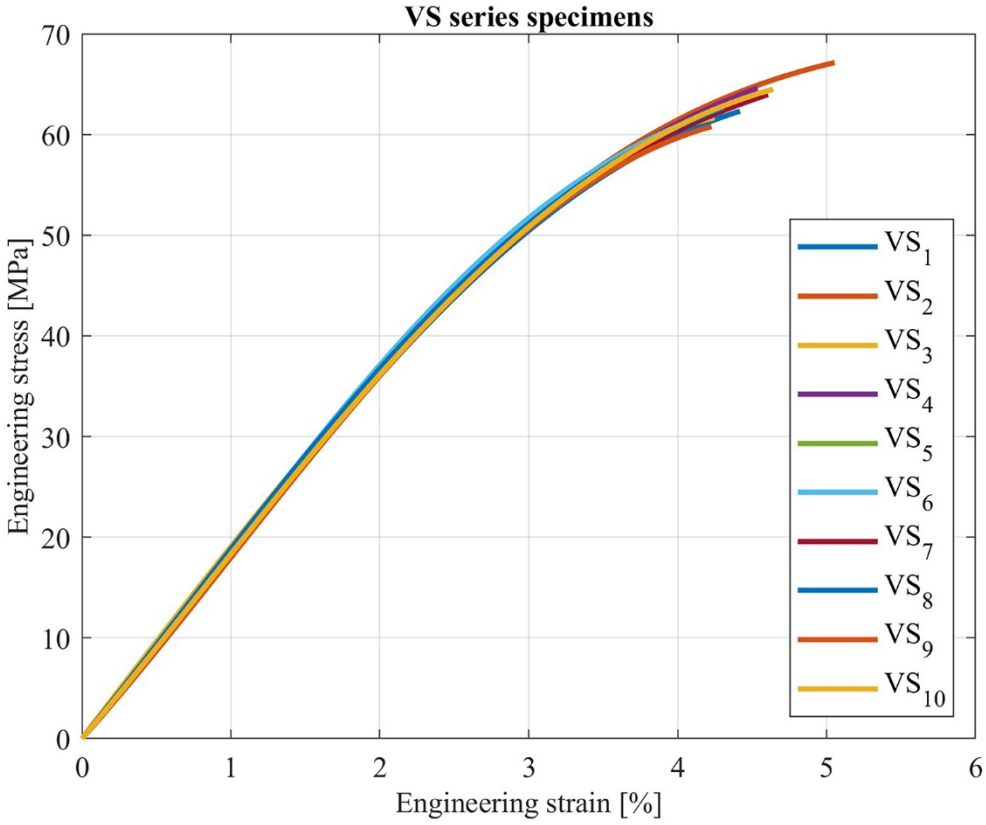


**Fig 9.** Dependence of engineering stress on the engineering strain for VS specimens.

As mentioned before, both horizontal and vertical specimens printed in the middle of the platform showed repeatable behavior, i.e. relatively good agreement between the specimens belonging to the same batch is obtained. The difference in maximum values of engineering stress parameter was around 20 % in favor of horizontal printed specimens in the middle of the powder bed; both specimens (i.e. horizontal and vertical specimens printed in the middle of the powder bed) exhibit different values of engineering strain at maximum force. The difference in maximum values of engineering strain is 30% in favor of horizontal specimens printed in the middle of the powder bed.

## 4. Conclusions

This paper presents the results obtained by examining 3-point bending specimens. They were fabricated by selective laser sintering from polyamide PA12. The examination of these additively produced specimens enabled the determination of the mechanical characteristics of these specimens printed in different print orientations and at different locations. The results of examination of the 3-point bending specimens printed by SLS indicate that the mechanical characteristics of the printed components vary significantly with the print orientation and location. The specimens printed horizontally in the middle of the powder bed exhibit higher engineering stress values than the vertically printed specimens in the same location.

Furthermore, the results obtained in this study are repeatable, indicating the consistency and reliability of the testing method used. The findings of this research can aid in the optimization of the

printing process parameters to produce components with desired mechanical properties. The knowledge gained from this study can also help in the design of SLS-printed components to ensure their mechanical integrity and reliability.

The results of this research can also be used to identify opportunities for the application of SLS printing in specific industries or applications. For example, the higher strength values observed in horizontally printed specimens could be beneficial in applications that require components to withstand high loads or stresses.

Additionally, the findings of this study could also be used to develop design guidelines and standards for SLS-printed components. These guidelines could specify the minimum requirements for mechanical properties based on the intended application and print orientation.

In conclusion, the results of this study have significant implications for the additive manufacturing industry, and further research in this area can have a significant impact on the design and production of high-performance components. The continued development and optimization of SLS printing processes can enable the production of complex geometries and unique designs that were previously not possible with traditional manufacturing techniques, making it an attractive option for various industries.

## Acknowledgments

The authors acknowledge the support from the Ministry of Education, Science and Technological Development of the Republic of Serbia (contracts: 451-03-47/2023-01/200213).

The authors are grateful to the company “3D Republika” for providing all specimens used in this research.

## 5. References

1. I. Gibson, D. Shi, Rapid Rapid Prototyping Journal, 3, No. 4, (1997), p. 129-136.
2. A. Milovanović, A. Sedmak, Z. Golubović, K. Zelić Mihajlović, A. Žurkić, I. Trajković, M. Milošević, Journal of the Mechanical Behavior of Biomedical Materials, 119 (2021).
3. W. Han, L. Kong, M. Xu, International Journal of Extreme Manufacturing, 4, no. 4, (2022).
4. I. Jevtic, G. Mladenovic, M. Milosevic, A. Milovanovic, I. Trajkovic, M. Travica, Structural Integrity and Life, 22, no. 3, (2022), p. 288-292.
5. “ASTM F2792-12a: Standard Terminology for Additive Manufacturing Technologies” () .
6. F. Christakopoulos, P. M. H. van Heugten, T. A. Tervoort, Polymers, vol. 14, (2022).
7. R. Brighenti, M. P. Cosma, L. Marsavina, A. Spagnoli, M. Terzano, Journal of Materials Science, 56, (2021), p. 961-998.
8. R. Leal, F. M. Barreiros, L. Alves, F. Romeiro, J. C. Vasco, M. Santos, C. Marto, The International Journal of Advanced Manufacturing Technology, vol. 92, (2017), p. 1671-1676.
9. Q. Yan, H. Dong, J. Su, J. Han, B. Song, Q. Wei, Y. Shi, Engineering, 4, (2018), p. 729-742.
10. S. C. Ligon, R. Liska, J. Stampfl, M. Gurr, R. Mülhaupt, Chemical reviews, 117, no. 15, (2017), p. 10212-10290.
11. H. Gong, K. Rafia, H. Gu, T. Starr, B. Stucker, Additive Manufacturing, 1-4, (2014), p. 87-98.
12. S. Rouf, A. Malik, N. Singh, A. Raina, N. Naveed, M. I. H. Siddiqui, M. Ir. U. Haq, Sustainable Operations and Computers, 3, (2022), p. 258-274.
13. A. Haleem, M. Javaid, S. Khan, M. I.Khan, International Journal of Industrial and Systems Engineering, 36, no. 3, (2020).

14. S. Moylan, J. Slotwinski, A. Cooke, K. Jurrens, M. A. Donmez, Journal of Research of the National Institute of Standards and Technology, 119, (2014), p. 429-459.
15. R. D. Goodridge, C. J. Tuck and R. J. Hague, Prog. Mater. Sci., 57 (2012) 229-267.
16. G.V. Salmoria, J.L. Leite, L.F. Vieira, A.T.N. Pires, C.R.M Roesler, Polymer Testing 31 (2012) 411–416.
17. A.A.M. Damanhuri, A. Hariri, S. Ab Ghani, M.S.S. Mustafa, S.G. Herawan, N.A. Nuur Azreen Paiman, International Journal of Environmental Science and Development, 12, No. 11.
18. R.J. Wang, L. Wang, L. Zhao, Z. Liu, International Journal of Advanced Manufacturing Technology, 33,(2007), p. 498–504.
19. A. Pilipovic, T. Brajlih, I. Drstvenšek, Polymers, 10, (2018).
20. C. Kundera, T. Kozior, XIII International Conference Electromachining, (2018), p. 020012-1 – 020012-7
21. H. Schappo, L. Piaia, D. Hotza, G., V. Salmoria, Materials Science Forum, 1012, (2020), p. 278 – 283.
22. G.V. Salmoria, V.R. Lauth, M.R. Cardenuto, R.F. Magnago, Optics & Laser Technology, 98, (2018), p. 92-96.
23. I. Trajkovic, M. Milosevic, M. Travica, M. Rakin, G. Mladenovic, Lj. Kudrjavceva, B. Medjo, Science of Sintering, 54, (2022) , p.373-386.
24. Martynková G.S., Slíva A., Kratošová G., Barabaszová K.C., Študentová S., Klusák J, Brožová S., Dokoupil T., Holešová S. Polymers, 13, (2021).
25. T. R. Crompton, Engineering Plastics, (2014).
26. A. Touris, A. Turcios, E. Mintz, S.R. Pulugurtha, P. Thor, M. Jolly, U. Jalgaonkar, Results Mater. 8, (2020).
27. Formlabs.com.:https://formlabs-media.formlabs.com/ datasheets/ 2001447-TDS-ENUS-0.pdf (Accessed on 25 April 2023).
28. Shimadzu.com:https://www.ssi.shimadzu.com/products/materials-testing/uni-ttm/autograph-ags-x-series/spec.html (Accessed on 25 April 2023).
29. M. Milosevic, N. Milosevic, S. Sedmak, U. Tatic, N. Mitrovic, S. Hloch, R. Jovicic, Technical Gazzete, 23, (2016), p. 19-24.
30. M. Milosevic, N. Mitrovic, R. Jovicic, A. sedmak, T. Maneski, A. Petrovic, T. Aburuga, Chemicke Listy, 106, (2012), p. 485-488.
31. N. Mitrovic, M. Milosevic, N. Momcilovic, A. Petrovic, A. Sedmak, T. Maneski, M. Zrilic, Chemicke Listy, 106, (2012), p. 491-494.
32. I. Tanasic, Lj. T. Sojic, N. Mitrovic, A. M. Lemic, M. Vukadinovic, A. Markovic, M. Milosevic, Measurement, 72, (2015), p. 37-42.
33. M. Lezaja, Dj. Veljovic, D. Manojlovic, M. Milosevic, N. Mitrovic, Dj. Janackovic, V. Miletic, Dental Materials, 31, (2015), p. 171-181.
34. N. Mitrovic, A. Petrovic, M. Milosevic, N. Momcilovic, Z. Miskovic, T. Maneski, P. Popovic, Chemical Industry, 71, no. 3, (2017), p. 251-257.
35. I. Martic, A. Sedamk, N. Mitrovic, S. Sedmak, I. Vucetic, Technical Gazette, 26, no. 3, (2019), p. 852-855.